

**MASSACHUSETTS INSTITUTE OF TECHNOLOGY
HAYSTACK OBSERVATORY
WESTFORD, MASSACHUSETTS 01886**

June 1, 2011

To: Broadband Development Group

From: C. J. Beaudoin, S. Cappallo

Subject: MOBLAS7 and NG SLR Radar Power Level Measurements Collected at GGAO

1. Summary

Power level measurements of the NG and Moblas7 SLR aircraft tracking radar systems were collected at GGAO in support of collocating the VLBI and SLR techniques at the space geodesy integrated station. These measurements were compared to theoretical expectations and good agreement was observed when the radar system was configured in a manner similar to that in which the radar's radiation patterns were measured. Significant deviations of the measured power levels from expectation were observed when the radar was configured in its operational state.

2. Introduction

The aircraft tracking radars incorporated with the NG and MOBLAS7 SLR systems pose a concern to the operational performance and health of the 12m VLBI2010 (GV12) radio telescope installed at the GGAO. The cause for concern is due to the strong X-band (9.4 GHz) aircraft tracking radars transmitting a peak EIRP of *100 dBm* in close proximity to GV12. The GV12 receiver front-end incorporates very sensitive microwave electronics having an input saturation point of approximately -50dBm; both SLR systems incorporate the same radar (*Raytheon R20XX*). In the case of MOBLAS7, the radar standoff range to GV12 is 160m and that of the NGSLR radar is 200m.

In order to avoid operational conflicts between these two systems, both scheduling and shielding (i.e. physical barrier) techniques are being considered to avoid excessive reception of the radar signal by GV12. The details of these mitigation strategies will not be discussed here, however, both of these proposed solutions rely on an understanding of the radar's radiation behavior. The focus of this memo will be on the radar power level measurements conducted at the GGAO on March 7-9, 2011 which were done to confirm our understanding of the radars' radiation behavior based upon information documented in [1].

3. Experimental Setup

3a. Site Layout and Geometrical Considerations

Figure 1 displays an aerial photo of GGAO showing the locations of both radar systems as well as the two locations where radar power level measurements were collected. Table 1 provides the surveyed latitude, longitude, and altitude of each location shown in Figure 1 as well as the standoff range to each point of reception. The locations where power level measurements were collected are sufficiently far from each transmitter that the far-field requirement is satisfied as outlined in Appendix 1.

3b. Receiver Configuration and Calibration

Figure 2 displays the receiver setup used to acquire the radar waveform and obtain peak power measurements. In this setup the DPO7254 oscilloscope was configured as a simultaneous fft analyzer such that the display reported the spectrum of the waveform within the time span window of the oscilloscope trace. The oscilloscope was configured to report the power at 540 MHz during the power level measurement verification performed at Haystack and 940 MHz for calibration and radar power measurements at GGAO¹; this is the oscilloscope total power quantity reported in this document. Lastly, the channel input impedance was set to 50 ohms so that all voltage trace measurements can be easily converted to power using the traditional 50 ohm system impedance.

Also shown in Figure 2 is a microwave pulsed/CW reference signal generator comprised of an Agilent E8257 synthesizer, a HP33124A microwave PIN switch and, a 2-18 GHz high pass filter². This pulsed/CW generator served as a power level reference which was used to calibrate the gains/losses in the receiver so that IF power level measurements made in the backend could be referred to the RF levels at the front-end of the cascade. During the actual radar power measurements the pulse/CW calibration hardware was left in the cascade to avoid the need to recalibrate the hardware; in this case the switch was simply left in the low-insertion-loss state.

An accounting of the gains/losses in the RF signal path is given in Table 2. The calibration process was conducted twice: once in the laboratory at Haystack and a second time at GGAO. The first calibration was performed as part of a pre-experiment verification to demonstrate that the proposed peak-power level measurement setup yielded accurate results. The second calibration was performed on-site at GGAO with the necessary power-limiting attenuators (see section 3c) installed in the cascade. Since the receiver was set up with slight differences at Haystack and GGAO, (i.e. different cables, attenuators etc.), it was necessary to repeat the calibration process on-site. The gain/loss budget for each setup is also outlined in Table 2.

During the power level measurement verification process conducted at Haystack the pulse generator was setup to modulate the 9.0 GHz -20.0 dBm CW signal with parameters nearly equivalent to those of the radar waveform (i.e. 1 microsecond pulse at

¹ During the calibration procedure executed at Haystack, the frequency of the radar was assumed to be 9 GHz as opposed to the actual frequency of 9.4 GHz.

² The high pass filter served to filter out transients of the switching signal that coupled directly into the into the RF transmission line.

660 Hz PRF). Given the pulsing parameters, the difference between the time-average power of the tone at 540 MHz and the instantaneous peak power levels of the pulse, Δ_{pow} , is given by:

$$\Delta_{pow} = 20 \log_{10}(\tau_p f_{prf}) \quad (2)^3$$

where τ_p is the pulsewidth(seconds) and f_{prf} is the pulse repetition frequency (Hz). Given the pulse parameters for this experiment $\Delta_{pow} = 63.6 \text{ dB}$.

Figures 3 and 4 display the oscilloscope and spectrum analyzer traces, respectively, collected during the calibration process. In Figure 3 the oscilloscope shows a peak power of -16.8 dBm (Figure is best viewed in electronic format with zoom) which is the expected power level given the -20.0 dBm level of the synthesizer plus the aggregate gain (3.1 dB) of receiver cascade given in Table 2. The spectrum analyzer measurement shown in Figure 4 displays an -80.8 dBm average power measurement of the 540 MHz carrier frequency; this level is 63.1 dB below the peak level which is within 0.5 dB of the expectation. The spectrum analyzer was used during the calibration process as a secondary means to confirm the calibrated total power measurements made with the synthesizer/oscilloscope. In the actual radar power level measurements, readings were not collected from the spectrum analyzer (see appendix 2).

3c. Transmitter/receiver antenna characteristics and pointing determination

Figure 5 displays a photo of the MOBLAS7 radar with the radome removed. Electromagnetic theory of standard waveguide bands dictates that the short edge of the waveguide is parallel to the electric field (polarization) vector in the TE_{10} mode of operation. Therefore, since the short edge of the waveguide feeding the reflector antenna is perpendicular to the ground plane at 0° elevation, the radar transmits vertical polarization. Figure 6 is a replication of the measured E-plane pattern of the radar antenna taken from Figure 16 in reference [1]. By definition, the E-plane contains the direction of wave propagation and the electric field vector (i.e. vertical polarization), hence, this E-plane pattern is the radiation behavior one would expect to measure if the radar were pointed azimuthally at a vertically-polarized receiver while sweeping the elevation angle. Otherwise put, the horizontal axis of Figure 6 can be regarded as elevation angle given the operational orientation of the radar. Also, Figure 6 displays the normalized gain (i.e. relative to boresite), so one must add 35.2 dB (i.e. boresite gain of the antenna) to obtain the absolute gain of the radar at a particular elevation angle. Figure 6 also displays an asymmetric pattern and there is not enough information available (at least to us) to discern which side of boresite (i.e. positive or negative elevation angle) has the weaker sidelobe.

Figure 7 is a photo of the experimental setup used at GGAO to make the radar power level measurements. A Scientific Atlanta standard gain horn model 12-8.2 was used as the receiving antenna and was mounted on a surveyor's tripod incorporating a custom azimuth/elevation mount for pointing adjustment. The mount was used simply as

³ The peak and average power of a pulse are related through the duty factor $\tau_p f_{prf}$ such that $P_{peak} = P_{avg} \tau_p f_{prf}$. In this case, P_{avg} is the sum of the power contained in all harmonics which is not the situation considered in equation 2. In this equation, it is only the time-average power in the harmonic at the carrier frequency (i.e. 540 MHz) that is considered.

a means of articulating the horn independently in azimuth and elevation without inadvertently rotating the polarization sense of the horn which was oriented to receive the vertical polarization. The mount was not graded for azimuth and elevation pointing⁴, hence, pointing information was not available from the receive mount. Instead, the receiver pointing was adjusted independently in azimuth and elevation to maximize power reception for a given transmitter pointing.

The peak power level of the radar transmitter on boresite is considerably greater than the operating capabilities of the receiver hardware; the UDC output signal saturates by 1dB when the input signal is ~ -15 dBm. Hence, received power level measurements were conducted on the second sidelobe of the antenna's radiation pattern where the power levels are 28-32 dB, (because of aforementioned sidelobe ambiguity) lower than those on boresite. In this way, we were able to keep the received power levels within the safe operating capabilities of the receiver hardware.

3d. Calculation of expected radar power levels

The expected power levels are calculated based on the Friis transmission formula:

$$P_{receive} = 10 \log_{10} \left(P_t G_t G_r \left(\frac{c}{4\pi f R_s} \right)^2 \right) \quad (3)$$

where P_t is the peak power of the radar transmitter (66.0 dBm per [1]), G_r is the gain of the receive antenna (MI Technologies⁵ model 12-8.2 22 dBi at 9.4 GHz [2]), R_s is the standoff distance between the transmitter and receiver from Table 1, and G_t is the gain of the transmitter in the direction of the receiver. Given that the boresite gain of the radar antenna is 35.2 dBi per [1] and that measurements are being made on the 2nd sidelobe of the elevation pattern (Figure 6) which is 28-32 dB lower than the boresite gain, the gain in the direction of the receiver is 3.2-7.2 dBi. Given these parameters the expected power levels were calculated and are shown in Table 3. Since we expect to observe ~ 0.0 dBm at the output port of the standard gain horn, a 38 dB attenuator was inserted in the front-end to accommodate the input range of the updown converter as shown in Figure 2.

3e. Transmitter Pointing

A coarse radar-to-receiver pointing was determined by the radar operator with the rifle scope mounted on the side of the radar dish as shown in Figure 5. The scope is offset approximately one-meter from the vertex of the dish so the geometric pointing error introduced by this offset is less than the width of the 2nd sidelobe in the closest observation (i.e. Mob7 to GODEW). After boresite pointing was identified with the rifle scope the antenna was raised 10.5° elevation relative to the boresite elevation in order to

⁴ The elevation axis on the receiver mount did incorporate an elevation level which could be used to measure elevation pointing but not to better than a degree.

⁵ The horn used in the experiment was a Scientific Atlanta SGH. However, the microwave component of Sci Atlta was absorbed by MI Technologies, and only MI Tech. data sheets were able to be located but assumed to contain identical data on the SGH.

reach the second sidelobe of the E-plane pattern; the purpose for pointing on the second sidelobe is explained in section 3c.

After the coarse pointing was complete, a fine azimuth and elevation peak search was performed to locate the azimuth/elevation point of maximum power reception on the 2nd elevation sidelobe of each radar antenna. This was done through coordination of the radar operator and the observer at the receiving location communicating with hand-held radios. The radar operator made a fine pointing angle adjustment and observer reported back as to whether or not the reception improved or degraded.

The MOBILAS7 pointing system possesses the capability to command pointing in azimuth and elevation with 0.1 degree precision. The NG SLR radar on the other hand does not have the capability to perform commanded pointing though encoder feedback was available to determine its absolute pointing. Therefore, in the case of the NG SLR radar, the operator was forced to nudge the pointing by what was intuitively the correct adjustment and then noted the encoder position in order to localize the pointing angles at which maximum reception of the local sidelobe was detected. Table 4 displays the azimuth/elevation pointing angles at which maximum power reception was detected for each location.

4. Measured Results

4a. GODEW Waveforms and Power Level Measurement

Figure 8 displays a 200ns, 50ns, and 2.5 ns oscilloscope traces of the MOBILAS7 radar transmit waveform in the absence of the radome and fall-protection railings with the receiver located at GODEW. Without going to the extent of removing the radar from the platform, this situation mimics most closely the conditions under which the antenna pattern shown in Figure 6 was measured. The waveforms in Figure 8 were measured at the back-end of the receiver depicted in Figure 2 after peaking the power reception on the 2nd sidelobe in the elevation pattern. There are no obvious signs of large voltage transients in the waveform, so it is permissible to calculate the peak power through the following process:

1. Calculate the rms voltage of the waveform during the on state
2. Convert the rms voltage to power dissipated into a 50-ohm load
3. Refer the back-end power measurement to the front-end using the cascade gain given in Table 2.

Following this process, an rms voltage of 36.4 mV is calculated from the trace data shown in Figure 8a, during the on state of the waveform. This represents -15.8 dBm into a 50 ohm load in the back-end and a received power level of -0.8 dBm referred to the front-end of the receiver given the cascade gain data provided in Table 2. This power level is within 1 dB of the expectation if receiving on the -28 dB 2nd sidelobe in Figure 6.

To understand what effect the operational conditions have on the receive power level, separate traces were collected with the radome in place, with the railings in place, and with both the railings and radome in place. These traces were collected at the identical pointing angles used to collect the traces shown in Figure 8, and no effort was

made to attempt to re-peak the reception. Figure 9 displays traces collected for the three aforementioned scenarios, and the measured power levels are summarized in Table 3.

4b. Location #2 Waveforms and Power Level Measurement

A similar sequence of measurements was also made at location #2. This site, unlike the GODEW site, also possessed a clear line-of-sight to the NG SLR radar so power measurements of this transmitter were made as well. The NG SLR, unlike MOB7, does not possess a large railing that obscures the line-of-sight to location #2 but rather had a small, horizontally-oriented wire that could not be removed, so it was present in all measurements of the NG SLR radar. Figure 10 displays traces collected while receiving the MOB7 radar transmission in the absence of the radome and railings, with the radome in place, and with both the radome and railings in place. Figure 11 displays traces collected while receiving the NG SLR transmission in the absence of the radome and with the radome in place. Table 3 summarizes the all measured power levels recorded at location #2.

5. Concluding Remarks

From the measured and expected power levels tabulated in Table 3, one can conclude that the measurements are within the uncertainty of their respective -28 and -32 dB SLLs when the operational provisions are removed. The fields to be compared have been color coded in Table 3 for ease of comparison. This result bestows faith in our understanding of the SLR aircraft-tracking radar's radiation properties. More testing would have to be conducted in order to eliminate the uncertainties regarding the sidelobe levels and improve the agreement between the measured and expected values in the absence of the radome and the railings. Such measurements would include re-measuring the antenna patterns to be sure of the true 2nd sidelobe level observed in the experiment. As a sanity check, it would also be useful to obtain a measure of the peak transmit power level. As reported in [1] (Table 2), the radar's peak power level is 4 kW but an uncertainty in this level is not provided. If it is mandated that the radiation properties of the radar must be known to better than 1dB (though a purpose is not clear), then such auxiliary tests will be needed.

When the radar is configured in its operational state, measurements of the radar power levels deviate significantly from both the expected levels and those levels measured when the radar was not operationally configured. This leads to the conclusion that the radome and railings are affecting the radar's radiation behavior. As such, it could be important to understand more about how the radar's radiation performance is affected by the operational provision (particularly with the Mob7 railings). An understanding of the influence of the railings could be avoided if they were simply removed for operations or if the radar was placed on a pedestal above the railings so as to circumvent their influence on the radar. The radome is a separate case.

Unlike the railings, removing the radome for SLR operations does not make logistical-sense, in some sense this defeats the purpose of the radome in the first place. However, the fact that the radome is affecting the power level measurements as shown in Table 3 is bothersome and suggests that there may be an issue with the integrity of the radome. Particularly irksome is the fact that the radome on Mob7 degrades the receive

power levels differently at each location while the NG SLR radome has an enhancing effect. Such behavior makes one suspicious that the radome is introducing multipath scattering into the experiment. A computational electromagnetic analysis of the radome's impact on the radar's free-space radiation pattern is the most feasible method of determining if the radome's influence is the expected. If it is determined by such analysis that the radome's influence is unexpected, then perhaps the design of a new radome is warranted. On the other hand, if the analysis reveals that this behavior is to be expected, then a more fitting model of the expected power level (i.e. modifying equation 3) should be developed for collocation analysis.

	N. Latitude (dms)	W. Longitude (dms)	Altitude (m)	Standoff Range (m)	
				To Mob7	To NGSLR
MOB7 radar	39° 1' 14.2229"	76° 49' 40.0015"	57.689		
NG SLR radar	39° 1' 12.66"	76° 49' 38.83"	57.7		
GODEW	39° 1' 17.9935"	76° 49' 37.5048"	49.285	131.1	No LOS
Loc #2	39° 1' 13.9774"	76° 49' 32.2777"	50.427	186.1	162.9

Table 1: Tabulated geometrical information on the transmitter and receiver locations considered in the GGAO SLR radar power level measurements

	Calibration at Haystack	Calibration at GGAO
Front-end Cable/Attenuator	-21.0 dB @ 9.0 GHz	-38.8 dB @ 9.4 GHz
Filter/Switch	-0.9 dB @ 9.0 GHz	-2.0 dB @ 9.4 GHz
UDC Gain	+29.0 dB @ 540 MHz	+29.0 dB @ 940 MHz
Splitter	-4.0 dB @ 540 MHz	-3.3 dB @ 940 MHz
Cascade Gain	+3.1 dB	-15.0 dB

Table 2: Gain/loss accounting for receiver test setup at Haystack and field setup at GGAO

	Expectation			Mob7 Measurements (dBm)				NG SLR Measurements (dBm)	
	SLL	Mob7 Radar	NGSLR Radar	No Obs	Radome	Railings	Radome Railings	No Obs	Radome
Loc#2	-28	-2.1	-1.0	-4.9	-7.0		-0.7	-3.6	-0.7
	-32	-6.1	-4.9						
GODEW	-28	1.0	No LOS	-0.8	-5.9	8.1	2.4	No Line of Sight	
	-32	-3.0							

Table 3: Summary of the expected power levels assuming sidelobe levels (SLL) of -28 and -32 dB owing to the ambiguity in the actual sidelobe used for observing in the experiment. Also, summarized are the measured power levels with no obscuration (No Obs), with radome, with railings, and with both radome and railings installed. The expected and measured power levels to be compared have been color coded for ease of identification.

	MOB7 radar	NG SLR radar
GODEW	(27.4°, 6.0°)	No LOS
Loc #2	(91.0°, 7.4°)	(76.1°, 7.9°)

Table 4: Radar azimuth and elevation pointing angles at which peak reception was detected on the 2nd sidelobe at each receive location. Pointing angles are reported as (AZIMUTH, ELEVATION)



Figure 1: Geographic layout of GGAO outlining locations of the MOBLAS7 and NG SLR radars (yellow markers) as well as GODEW and Loc #2 points (red markers) where power reception measurements were taken.

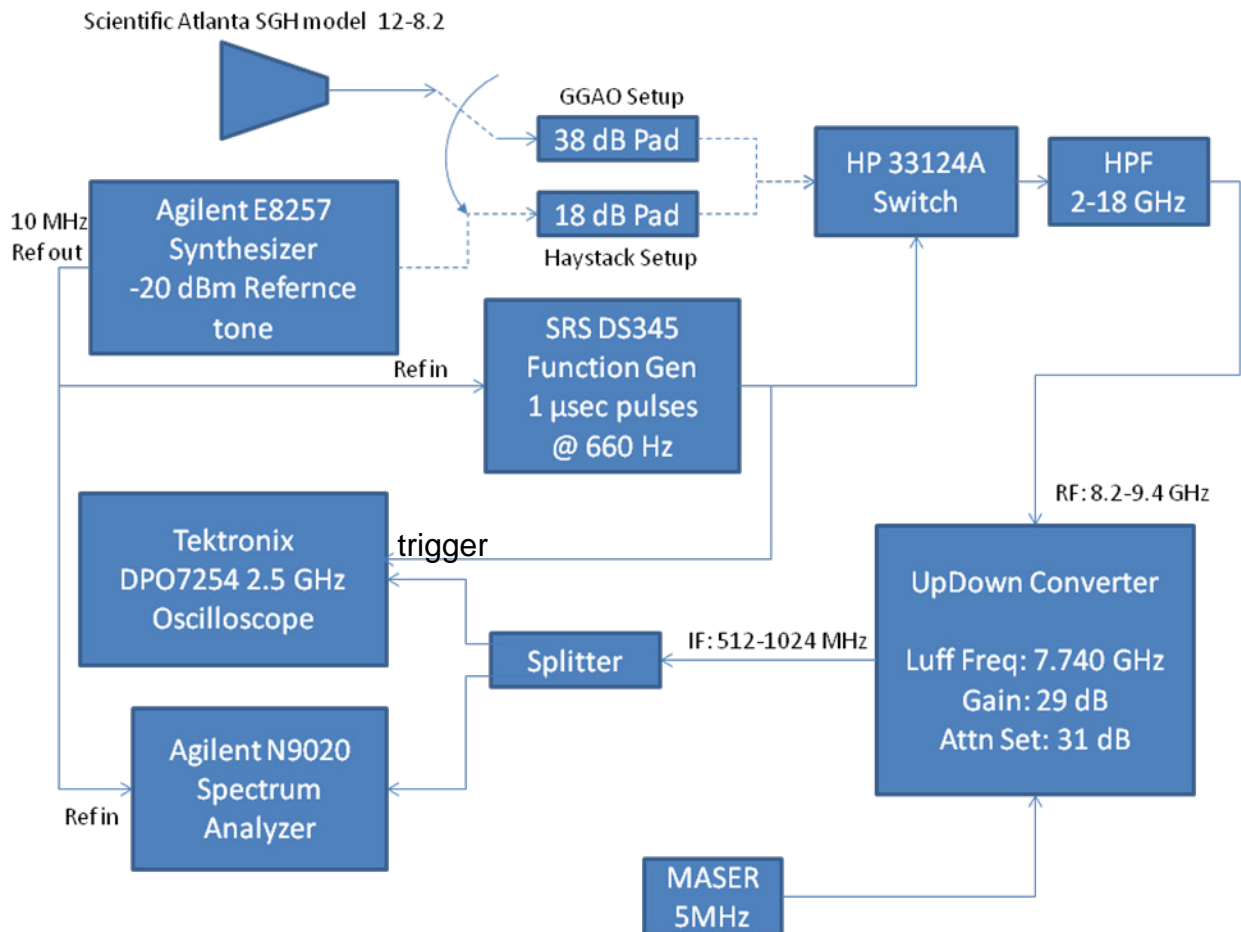


Figure 2: Block diagram of receiver used to perform radar power level measurements. The 18 dB attenuator was incorporated in the cascade to validate the measurement concept at Haystack. The 38 dB attenuator was incorporated in the cascade at GGAO, and the RF input was routed to the signal generator for calibration. During radar power level measurements, the HP33124A switch was set to the thru state. Operational specifications of the UpDown Converter (UDC) are given in [3]. The RF input bandwidth to the UDC is limited by the bandwidth of the X-band standard gain horn(SGH) and the UDC downconverts the input spectrum by $4f_{luff} - 22.5$ such that the radar pulse RF carrier frequency is translated to 940MHz.

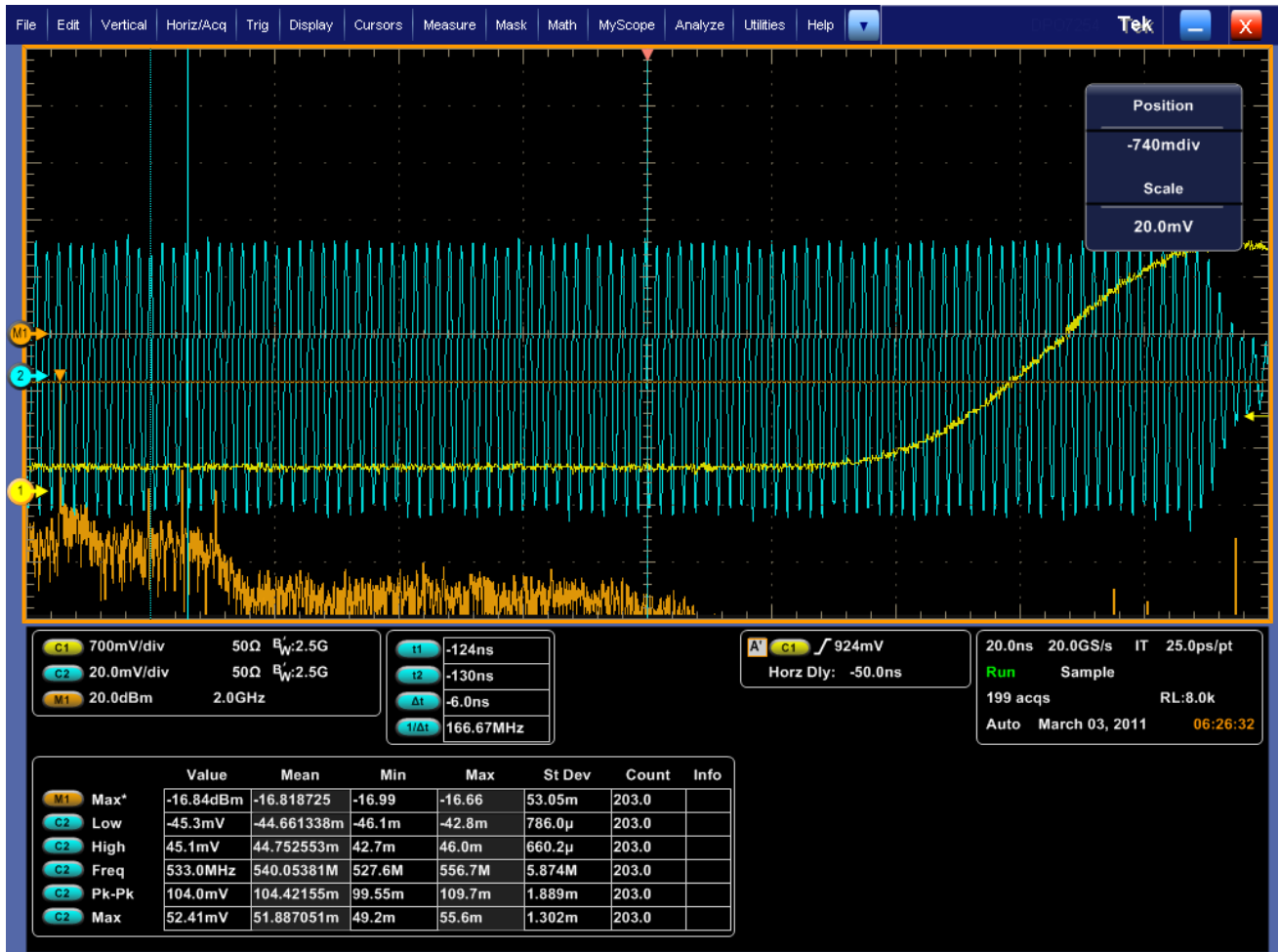


Figure 3: Oscilloscope traces captured for peak power level measurement verification.
 Blue trace: pulse/continuous 540 MHz waveform.
 Yellow trace: baseband pulse modulating the 540 MHz carrier.
 Orange trace: spectrum of the blue trace; the peak power reported by marker M1 is -16.84 dBm

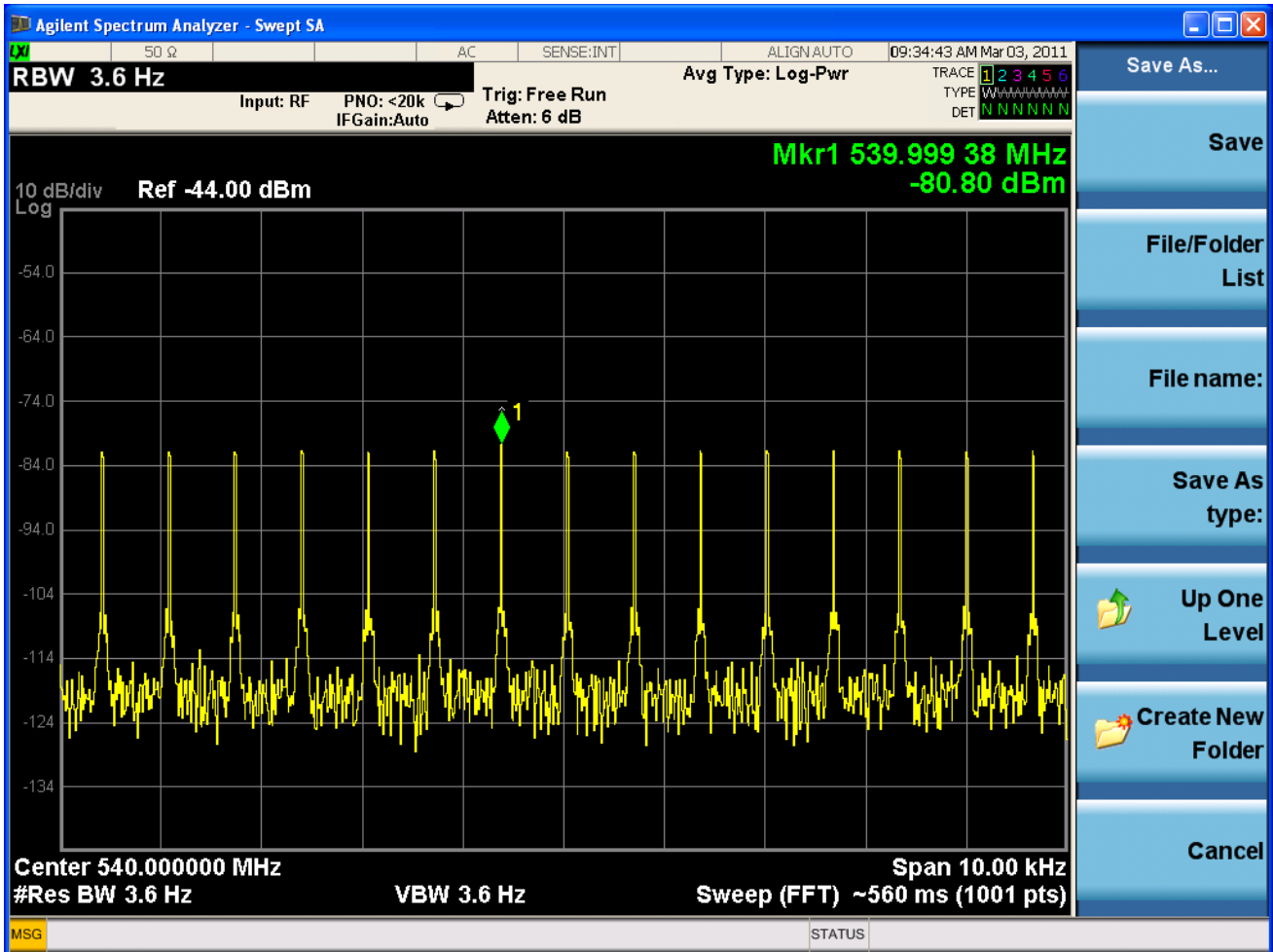


Figure 4: Spectrum analyzer trace showing 10 kHz span of the 540 MHz pulse signal spectrum centered at the carrier frequency. The spacing between harmonics of the pulse signal is the PRF (660Hz). The time average power of the rail at 540 MHz is reported by Mkr1 (-80.8 dBm).

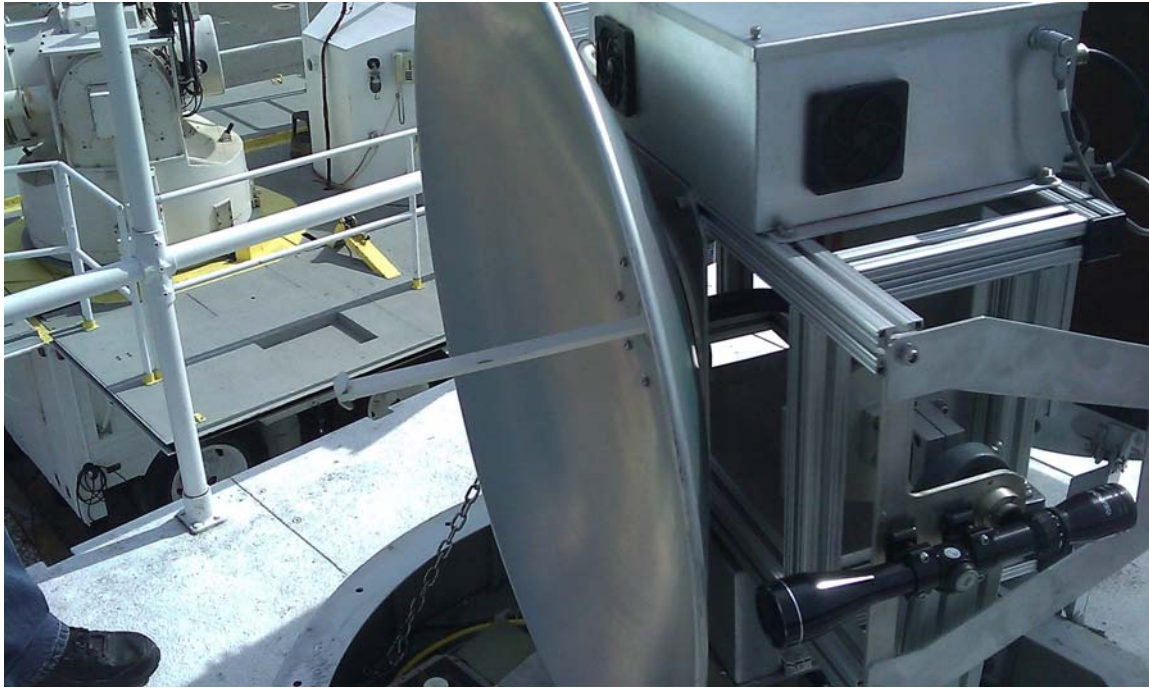


Figure 5: Photograph of Moblas 7 radar antenna. Also shown is the rifle scope used for pointing verification.

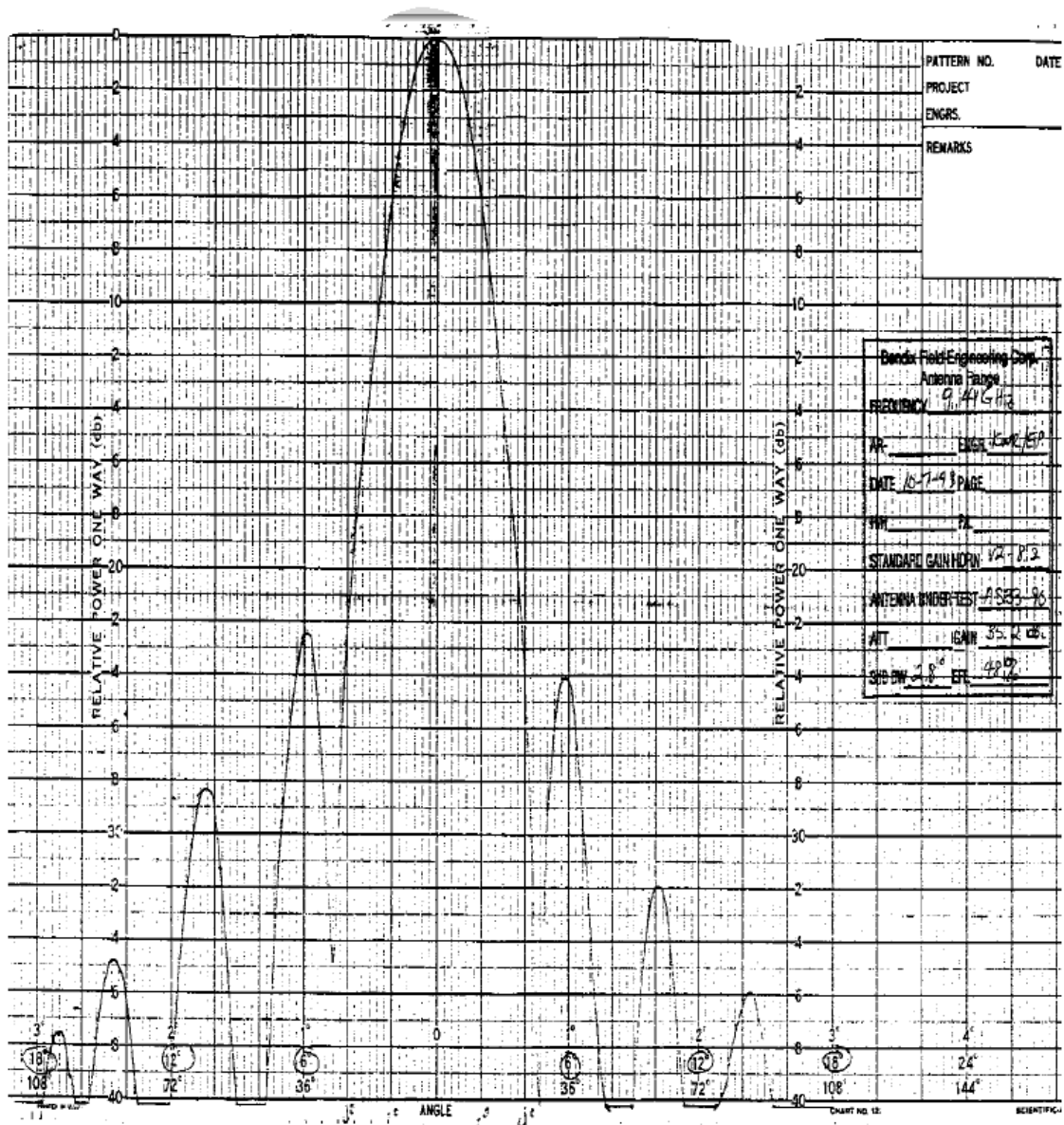


Figure 6: Measured E-plane pattern of the SLR radar antenna taken from [1]. Note the asymmetry in the 2nd sidelobe levels

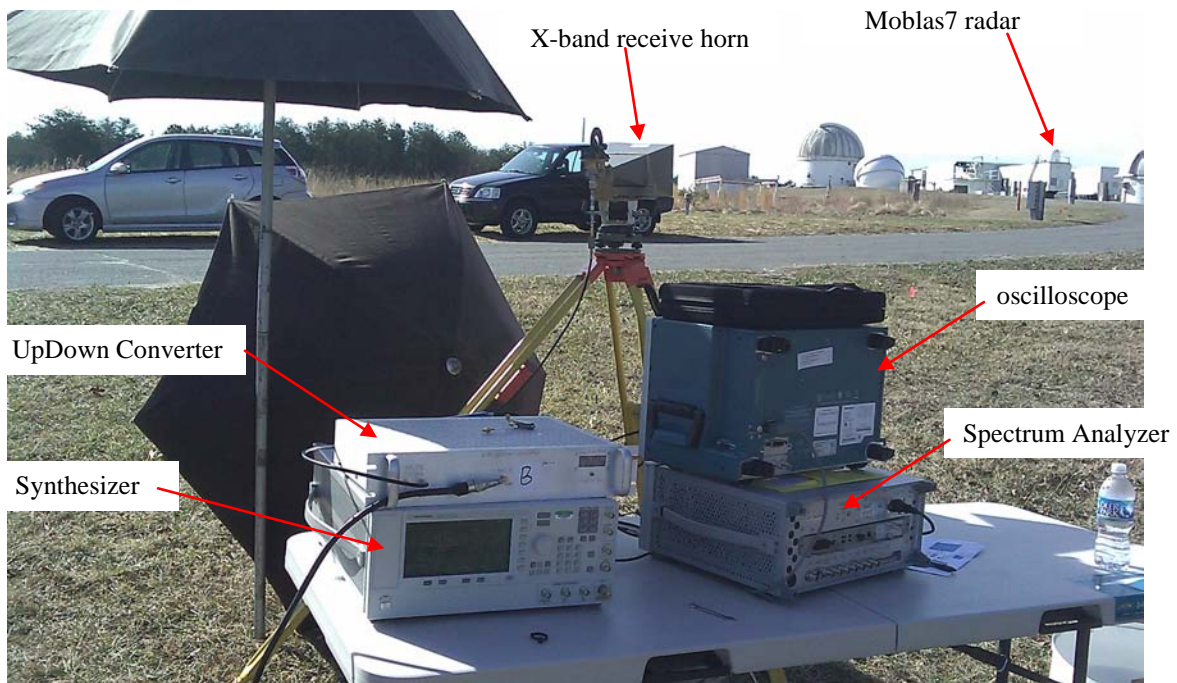
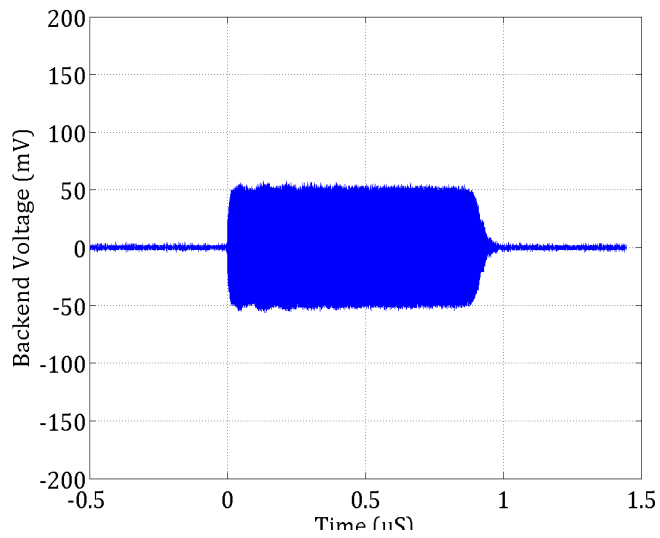
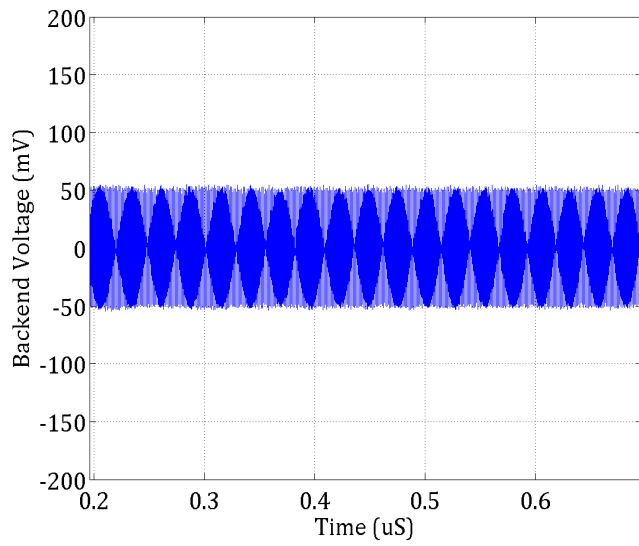


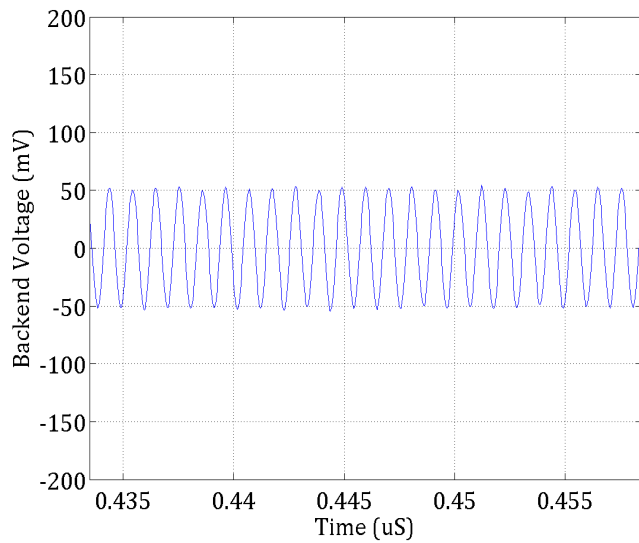
Figure 7: Photograph of receiver setup used to collect radar waveforms and peak power measurements. Location is GODEW.



(a)



(b)



(c)

Figure 8: Moblas 7 radar transmit waveforms received at GODEW location with radome and fall protection railings removed from the apparatus: (a) 2000 ns time window, (b) 500 ns time window and (c) 25 ns time window

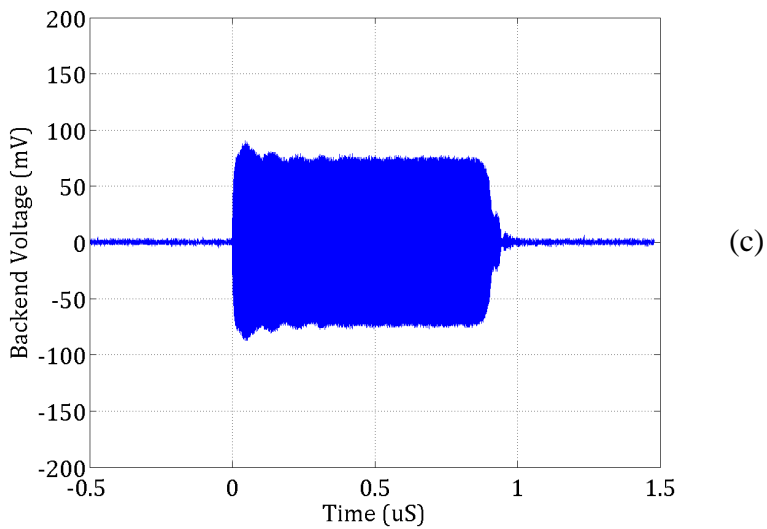
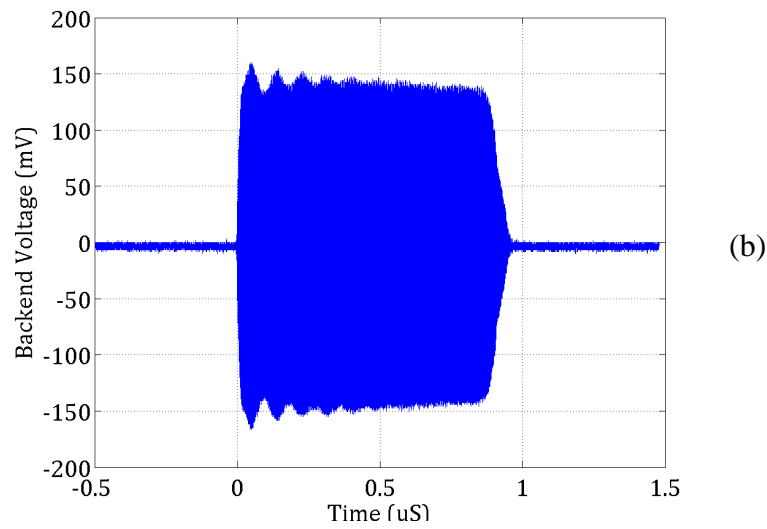
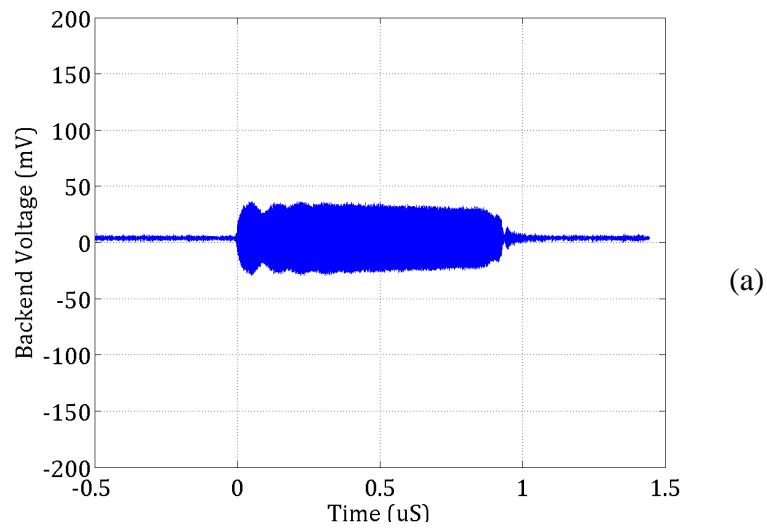


Figure 9: Moblas 7 radar transmit waveforms received at GODEW location: (a) radome installed (b) fall protection railings installed (c) both radome and fall protection railings installed

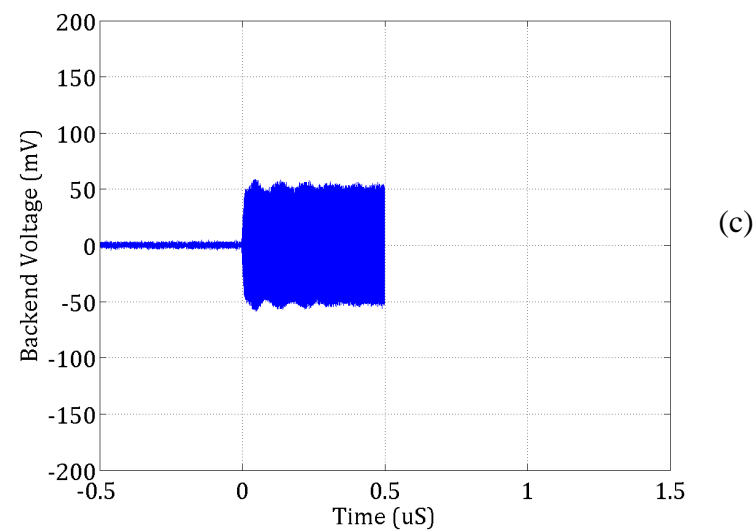
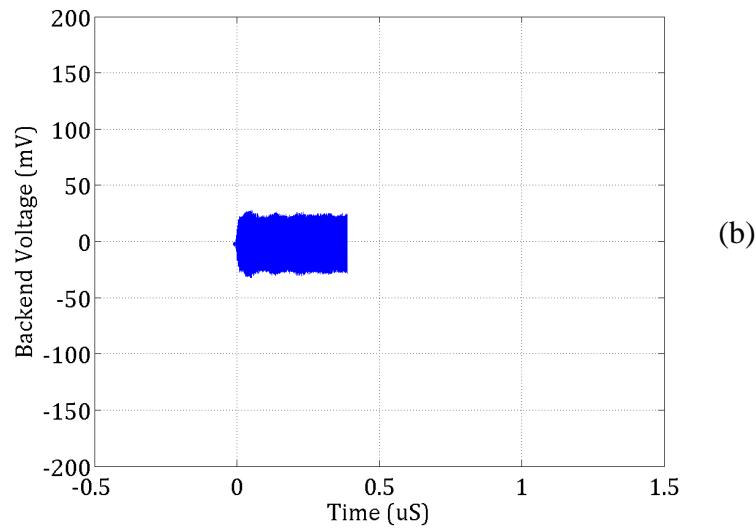
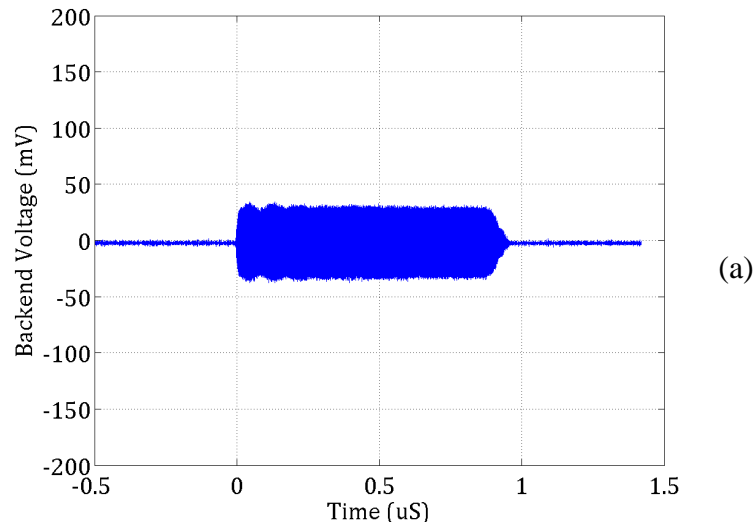


Figure 10: Moblas 7 transmit waveforms collected from location #2 with (a) radome and railings removed, (b) with the radome installed, and (c) with both the radome and railings installed. Note: waveforms (b) and (c) were truncated by the oscilloscope when stored, the cause has yet to be determined but the “on” state voltage level is easily discerned in all cases.

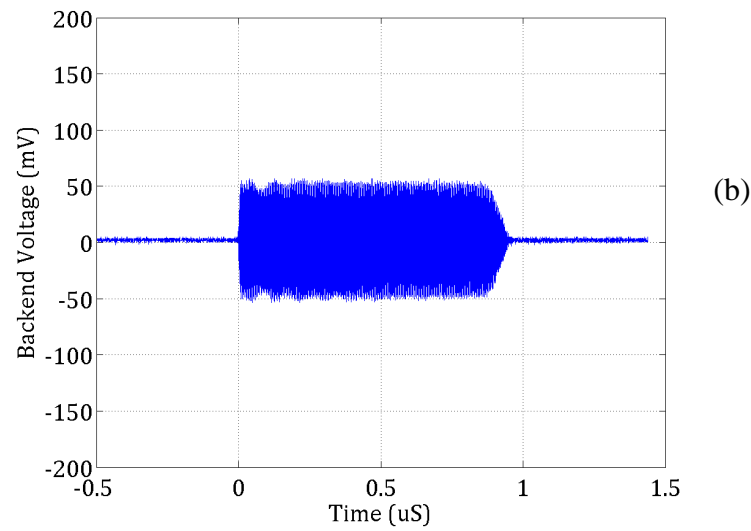
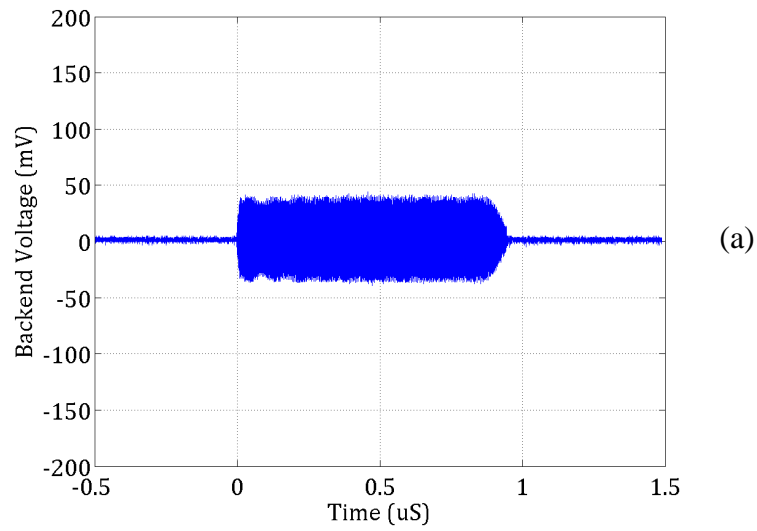


Figure 11: NG SLR radar transmit waveforms collected from location #2 with (a) radome removed and (b) with the radome installed.

Appendix 1: Far-field requirement for the power level measurements

The far-field requirement is imposed by the transmitting antenna since it is the largest of the two (receiver/transmitter) and this distance is given by:

$$R_{ff} = \frac{2fD^2}{c} \quad (1)$$

where R_{ff} is the far-field distance in meters, D is the diameter of the radar dish in meters, f is the radar frequency, and c is the speed of light. The far-field range for the 1-m radar dish radiating at 9.4 GHz is 62-m. From the information recorded in Table 1, we conclude that the stand-off range at both receiving locations is greater than R_{ff} .

Appendix 2 Rational Behind Oscilloscope Power Measurement

The oscilloscope was used to provide the primary power measurement because the lack of pulse-to-pulse coherency of the radar made it difficult to obtain an accurate total power measurement with the spectrum analyzer. Furthermore, the spectrum analyzer only reports average power and certain assumptions must be made about the shape of the radar waveform (e.g. pulsed/CW) in order to convert the average power measurement to a peak power estimate. It is important to note here that the peak power reception is critical knowledge regarding the health of the GV12 front-end. To our knowledge, the shape of the radar waveform is not documented and even if it were non-ideal operational circumstances can void such assumptions. Given the lack of apriori knowledge of the radar waveform, a time-average spectrum measurement was deemed unacceptable for assessing the peak radiated power levels. There are other spectrum analyzer techniques that could potentially provide an accurate peak power measurement (e.g. 0 Hz span bandwidth) but these other techniques were not explored.

References:

- [1] R.L. Allshouse, "Experimental Measurement of the Impact of NASA SLR Radar Emissions on VLBI Operations," Internal Memo, Honeywell Technology Solutions Incorporated, July 1997, Revision 2.
- [2] <http://www.mi-technologies.com/usefultools/gainhorn.pdf>
- [3] A.E.E. Rogers, "Performance Characteristics of UpDown Converter," MIT Haystack Observatory Mark 5 Memo Series, Memo #59, August 2010.
http://www.haystack.mit.edu/tech/vlbi/mark5/mark5_memos/059.pdf